

APPLICATION OF A NEW RACKING CYCLIC LOADING PROTOCOL ON COLD-FORMED STEEL-FRAMED WALL PANELS

Rojit Shahi¹, Nelson Lam², Emad Gad³, Ismail Saifullah⁴, John Wilson⁵ and Ken Watson⁶

ABSTRACT: *Resistance against lateral loads (due to wind or earthquake) in cold-formed steel-framed domestic houses is mainly provided by bracing wall panels. Behaviour of such cold-formed steel-framed wall panels under cyclic strain reversals in an earthquake is too complex to analyse and is best evaluated by physical experimentation. This paper presents racking tests of steel-framed wall panels with different aspect ratios sheathed with fibre cement board subjected to monotonic and new cyclic loading protocol. Monotonic test results showed similar strength per unit length of wall panels with various aspect ratios (provided that other parameters are not changed), however wall panels with higher aspect ratio revealed higher displacement capacity. Wall panels under cyclic loading showed highly pinched hysteresis response behaviour associated with significant stiffness and strength degradations at high displacement amplitude.*

KEYWORDS: Cold-formed steel-framed wall panels, racking tests, fiber cement board, new cyclic loading protocol

¹ Rojit Shahi, Department of Infrastructure Engineering, The University of Melbourne. Email: r.shahi2@pgrad.unimelb.edu.au

² Nelson Lam, Department of Infrastructure Engineering, The University of Melbourne. Email: ntkl@unimelb.edu.au

³ Emad Gad, Department of Civil and Construction Engineering, Swinburne University of Technology. Email: EGad@swin.edu.au

⁴ Ismail Saifullah, Department of Civil and Construction Engineering, Swinburne University of Technology. Email: Isaifullah@swin.edu.au

⁵ John Wilson, Faculty of Science, Engineering and Technology, Swinburne University of Technology. Email: JWilson@swin.edu.au

⁶ National Association of Steel-Framed Housing Inc (NASH), Australia. Email: kwatson@nash.asn.au

1 INTRODUCTION

Cold-formed steel (CFS) has been widely used in domestic low-rise buildings in industrialized countries including Australia. Commonly, CFS bracing wall panels (CFSBWPs) are the main vertical elements for resisting lateral loads (due to wind or earthquake) in this type of construction. A CFSBWP primarily consists of two elements; CFS frame and a bracing element. The CFS frame consists of studs placed at designated spacing and plates (or tracks) at top and bottom to interconnect the studs. Typically noggings are used to interconnect the studs at mid-height level to prevent buckling. For taller walls, two lines of noggings may be used. The bracing element may be strap bracing or sheathing (cladding) attached to the CFS frame on one or both sides typically using screws.

Racking strength and stiffness of a CFSBWP is primarily governed by the connections between the CFS frame and the bracing element, which is of complex behaviour [1-8] and is best evaluated by physical experimentation. This study presents experimental test results of CFSBWPs of different aspect ratios with fibre cement boards as the sheathing which was subjected to in-plane monotonic and cyclic loadings. As the performance of the wall panel is highly dependent on the cyclic loading protocol [9], a new loading protocol [10] which had been developed based on the seismic conditions of Australia [11], was used in this study for cyclic testing.

2 TESTING PROGRAM

2.1 SPECIMEN

Experimental studies were carried out on two different lengths (shown in Table 1) of wall panels braced with fibre cement boards. The wall panels were built from CFS framing members and fibre cement sheathing panels. The CFS frame was made of 89x36x0.75mm C-shaped lipped studs (with web stiffened) and 91x40x0.75mm plain channel sections for plates and noggings. Studs were placed at 600mm spacings for 2.4m long wall and 450mm spacings for 0.9m long wall. Two identical fibre cement boards [12] of 5mm thickness were used as the sheathing boards for 2.4m long wall whereas one board of 5mm thickness was used for 0.9m long wall. The sheathing boards were attached vertically on one face of the wall panel. All CFS members were grade G550 [13] and the connections between them were made using 15mm long M6 GX® Frame Screws [14]. The sheathing boards were connected to the framing members at 100mm spacings along the periphery of the board and at 150mm spacings for the middle portion of the board. All sheathing screws were 20mm long M5-16TPI CSK FibreZips self drilling screws [14].

Table 1: Matrix of test specimen

Specimen	Loading	Length (L)	Height (H)	Aspect Ratio
FCB-Mon-A	Monotonic	2.4m	2.4m	1.0
FCB-Mon-B	Monotonic	0.9m	2.4m	2.7
FCB-Cyc-A	Cyclic	2.4m	2.4m	1.0
FCB-Cyc-B	Cyclic	0.9m	2.4m	2.7

2.2 TEST SETUP AND INSTRUMENTATION

The experimental test setup is shown in Figure 1. The wall panel was assembled on the floor and was placed in the vertical position between the base beam (200UC52.2) at floor level and the spreader beam (100PFC) at the top. Base beam was anchored to the concrete floor by using M24 threaded rods spaced at 1000mm centres. Tie-down details between the bottom plate of the wall panel and the base beam were done as per guidelines given in [12]. Load was applied to the wall specimen via the spreader beam using a programmable hydraulic actuator. Castors were used along the spreader beam in order to prevent out of plane movement of the wall panel.

The instrumentation used during the tests is shown in Figure 1. The hydraulic actuator contained the internal LVDT (channel #1) and the load cell (channel #2) that supplied information on the applied displacement and resisting force. These two transducers supplied basic data for the load-deflection analysis of the tests. One linear displacement transducer (channel #3) was mounted at the right end of the top plate (opposite end of actuator) to measure top horizontal displacements. The amount of slip between the bottom plate and the base beam was measured by two LDT's (channel #4 and #5) mounted at each end of the bottom plate whereas two LDT's (channel #6 and #7) were placed at the bottom of each end studs to determine the end studs/bottom plate uplift and wall rotation. Information from channels #4, #5, #6 and #7 was used to account for wall slip and rotation while determining net deflection of the wall panel given by Equation (1):

$$\Delta_{\text{net}} = \Delta_3 - \frac{(\Delta_4 + \Delta_5)}{2} - (\Delta_6 - \Delta_7) \times \frac{H}{L} \quad (1)$$

where,

Δ_{net} = Net in-plane displacement due to fastener slip and shear deformation of the sheathing board

Δ_3 = Total in-plane displacement at the top of the wall panel measured by channel #3

$(\Delta_4 + \Delta_5)/2$ = Rigid body translation at the base (average of two readings from channel #4 and channel #5)

$(\Delta_6 - \Delta_7) \times H/L$ = Rocking displacement at the top due to rigid body rotation

H/L = Aspect ratio of the wall panel

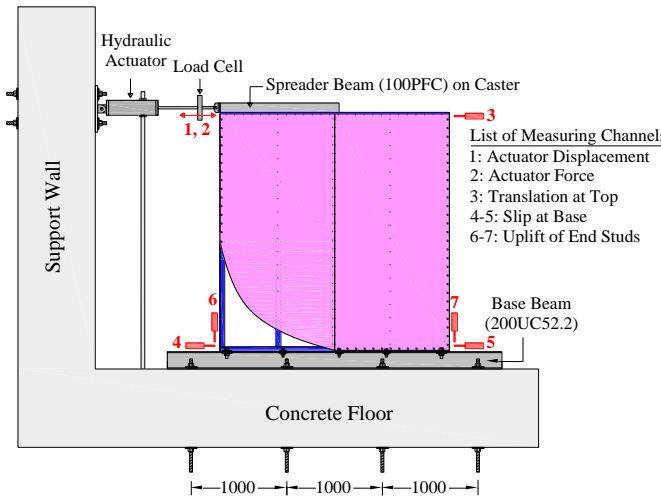


Figure 1: Test setup and instrumentation for racking test

2.3 LOADING

Two types of loading conditions were applied for the racking test; monotonic and cyclic loads. Monotonic loading was performed prior to the cyclic test to determine the displacement controlled parameter (Δ_M) which is a key parameter required for cyclic loading protocol [10] (shown in Figure 2). Displacement controlled parameter (Δ_M) refers to the displacement corresponding to 90% of the peak strength at the declining portion of the monotonic load deflection curve. The cyclic loading protocol used in the testing program was slightly modified from the loading protocol developed by Shahi *et al.* [10]. According to this loading protocol, wall panel was first subjected to four cycles in Phase 1 with displacement amplitude of Δ_1 , where Δ_1 refers to serviceable displacement which corresponds to 8mm (H/300) for a 2.4m wall height. Second Phase of the loading protocol consisted of four cycles with displacement amplitude Δ_2 and three cycles each in Phase 3 and Phase 4 with displacement amplitudes of Δ_3 and Δ_4 respectively. Increment of the displacement amplitude in each subsequent cycle was kept uniform for simplicity which is given by the following expression:

$$\delta = (\Delta_M - \Delta_1)/3 \quad (2a)$$

where,

Δ_M = Displacement corresponding to 90% of the peak strength at the declining portion of the monotonic load deflection curve

After finding the incremental displacement δ , displacement amplitude at any loading phase (n) can be determined from following expression:

$$\Delta_n = \Delta_1 + (n - 1)\delta \quad (2b)$$

All tests were conducted in the displacement controlled mode with a loading rate of 2 to 4mm/min for the monotonic tests and 4 to 16mm/min for the cyclic tests.

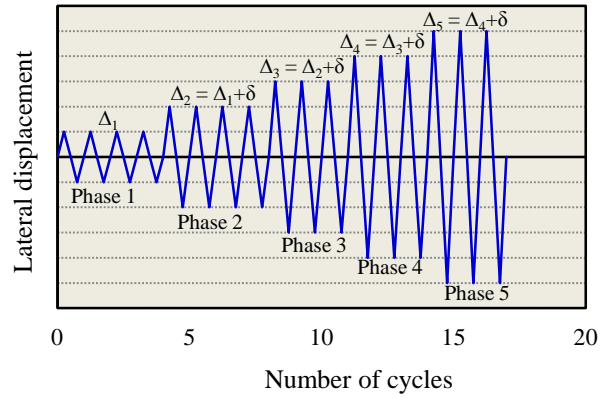


Figure 2: Modified cyclic loading protocol [10]

3 RESULTS AND DISCUSSION

3.1 FAILURE MODES

Most of the failure modes observed during the racking test of the CFSBWPs was associated with the connections of the board with the CFS framing members. Some observed local buckling of the top and bottom plates was recoverable. The sequence of the failure modes observed in the monotonic and cyclic tests are listed below:

- (a) Cracking of the board at the corners (BC): The diagonal corner cracking of the board occurred at early stages of loading (Figure 3a). A crack propagated along the end screws at the adjacent sides, at the two opposite corners of the board under tension, making the end screws ineffective in shear transfer.
- (b) Bearing failure of the sheathing board at edge screws (BB): Bearing failure was observed along the perimeter of boards with screw tilting and its head piercing down the sheathing material (Figure 3b). There was a very little or no damage of connections within the middle portion of board.
- (c) Screw head pull-through the sheathing board (BP): This failure mode was observed along the board edge (tension side overlapping edge) at the overlapping zone (Figure 3c).
- (d) Board edge tearing (BT): This failure mode was observed at some locations of the boards overlapping zone (Figure 3d).

Failure modes BP and BT led to the ultimate failure of the wall panel which was observed by the unzipping of the board edge (tension side overlapping edge) from the stud framing member. The separation of the board from the framing member led to the permanent rigid body rotation of the board relative to the framing members. The separation of the board from the framing members led to the permanent rigid body rotation of the board relative to the framing member as illustrated in Figure 4.

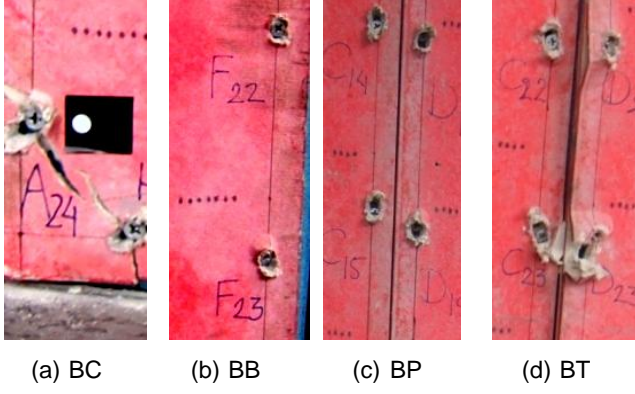


Figure 3: Observed failure modes during racking tests of wall panels

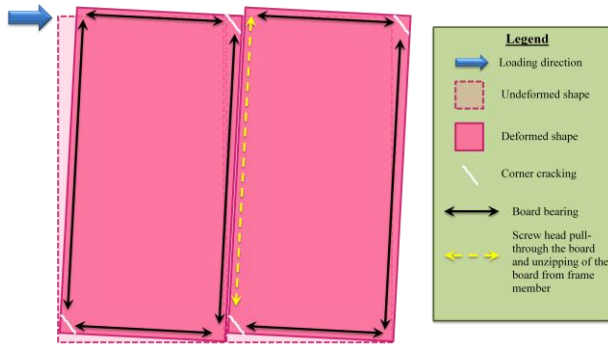


Figure 4: Schematic of the failure mechanism of wall panel under racking load

3.2 MONOTONIC TEST RESULTS

The load-deflection curves of the wall panels under monotonic tests for wall lengths 2.4m and 0.9m are shown in Figure 5. The X-axis of Figure 5 represents the net displacement (calculated using Equation (1)) and the Y-axis represents the load carried by the wall per unit length of wall. The general observations made from the monotonic load-deflection curves (Figure 5) are listed below:

- FCB-Mon-A is found to be stiffer (about 30%) than the shorter panel FCB-Mon-B. The reason for the lower stiffness of the shorter wall panel (with most likely aspect ratio of more than 2) is the larger bending deformation which is not significant in the longer wall (with aspect ratio equal to 1).
- Nonlinear behaviour in FCB-Mon-A starts at a load of around 60% of the ultimate load whereas nonlinearity starts at 40% of the ultimate load in the shorter panel FCB-Mon-B. The nonlinear behaviour in both wall panels was mainly due to deformations at the fasteners which connect the CFS framing members with the sheathing board.
- After reaching peak load, both wall panels undergo higher displacement without any further increase in load as illustrated by the plateau region in the load-deflection curve. This was primarily due to bearing of the fastener connections and screw head pull-

through the sheathing board as described in Section 3.1.

- Both wall panels possessed similar load carrying capacity per unit length of wall panel. Hence, load carrying capacity of wall panels of intermediate lengths can be estimated using linear interpolations. However, deflection capacity of the shorter wall panel FCB-Mon-B was found to be 25% higher than the longer panel FCB-Mon-A.

Both wall panels ultimately failed by the unzipping of the perimeter screws after reaching a moderate level of ductility (3 to 4). Important parameters from the load-deflection curves (Figure 5) such as stiffness (refer Figure 6), peak strength, deflection at peak strength, deflection at 90% of peak strength (Δ_M to be utilized in cyclic loading protocol) are provided in Table 2.

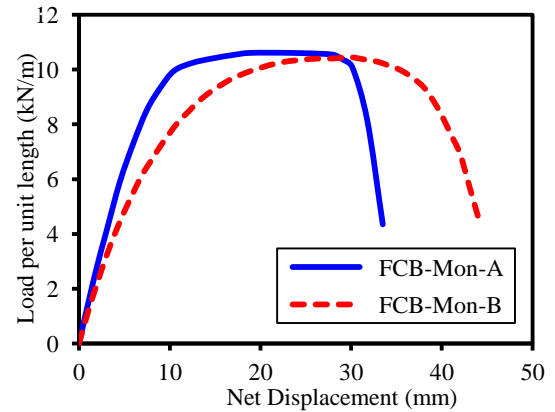


Figure 5: Load deflection behaviour of tested wall panels under monotonic loading

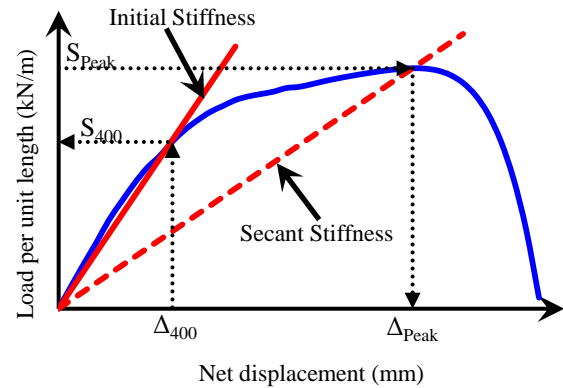


Figure 6: Definition of the initial and the secant stiffness for monotonic test

Table 2: Summary of monotonic test results

Specimen	Displacement controlled parameter Δ_M (mm)	Peak load per unit length S_{Peak} (kN/m)	Net racking displacement at Peak Load Δ_{Peak} (mm)	Initial stiffness per unit length (kN/mm/m)	Secant stiffness per unit length (kN/mm/m)	Failure sequence
FCB-Mon-A	30	10.9	23.4	1.21	0.47	BC+BB+BP+BT
FCB-Mon-B	37	10.5	27.9	0.92	0.38	BC+BB+BP

Table 3: Summary of cyclic test results

Specimen	Loading Phase	Net racking displ. Δ (mm)	Peak load per unit length (kN/m)		Load Degradation	Maximum residual displ. Δ_r (mm)	Δ_r/Δ	Effective stiffness per unit length (kN/mm/m)		Secant stiffness per unit length (kN/mm/m)		Failure sequence
			Virgin Cycle	Final Cycle				Virgin Cycle	Final Cycle	Virgin Cycle	Final Cycle	
FCB-Cyc-A	1	8.0	7.8	7.0	10%	2.5	0.31	1.16	1.10	0.98	0.88	BC+BB +BP+BT
	2	15.3	10.6	8.5	20%	5.7	0.37	0.94	0.90	0.69	0.55	
	3	22.7	10.2	7.7	25%	10.2	0.45	0.84	0.74	0.45	0.34	
	4	30.0	8.8	3.6	59%	15.0	0.50	0.72	0.27	0.29	0.12	
FCB-Cyc-B	1	8.0	5.7	5.1	9%	2.7	0.34	0.83	0.81	0.71	0.64	BC+BB +BP
	2	17.7	8.9	7.5	16%	6.1	0.35	0.80	0.76	0.51	0.43	
	3	27.3	9.7	6.9	29%	12.9	0.47	0.67	0.59	0.35	0.25	
	4	37.0	7.5	4.0	46%	17.5	0.47	0.49	0.26	0.20	0.11	

3.3 CYCLIC TEST RESULTS

Hysteretic behaviour of the wall panels under cyclic tests for FCB-Cyc-A and FCB-Cyc-B are shown in Figures 7a and 7b respectively. The X-axis of Figures 7a and 7b represents the net displacement (calculated using Equation (1)) and the Y-axis represents the load carried by the wall per unit length. The load-deflection hysteresis of both wall panels showed severely pinched loops with large residual displacement (displacement corresponding to zero load while unloading). This reflects that bearing of the fastener into the sheathing material was the primary mode of resistance. Important parameters such as peak load, residual displacement and stiffness were obtained for virgin and last cycles at each phase of loadings which are summarized in Table 3. These parameters were obtained from the average of positive and negative hysteresis loops. The load carrying capacity was degraded from the virgin cycle to the last cycle of loading at the same displacement amplitude (same phase) which is referred herein as 'load degradation'. For both wall panels, the test results showed a load degradation of less than 10% at first phase of loading ($0.25 \Delta_M$), 15 to 30% at second and third phases of loading ($0.50 \Delta_M$ and $0.75 \Delta_M$) and a severe load degradation (about 50%) at final phase of loading. As per [15], the residual displacement after each cycle is a function of the maximum displacement at that cycle. Results shown in Table 3 for both wall panels showed a reasonably constant residual displacement ratios; 0.31 to 0.38 before reaching peak loads and 0.45 to 0.50 for post peak loadings. Residual displacement is an important parameter while evaluating wall parameters and must not

exceed the wall plumb line tolerance limit at serviceability limit state. The residual displacement at serviceability limit state (at displacement of $H/300$) of the tested wall panels satisfied the tolerance limit set by the NASH Standard, Australia [16].

Two approaches were used to calculate the stiffness; (i) effective stiffness and (ii) secant stiffness as illustrated in Figure 8. The effective and secant stiffnesses for the wall panels at virgin and last cycles of each loading phase are provided in Table 3. For both wall panels, the secant stiffness was found to be substantially lower than the effective stiffness with increasing displacement amplitudes (about 1.5 times for first 2 phases of loadings and more than 2 times for final two phases of loadings). Test results also showed substantial amount of stiffness degradation (both effective and secant stiffness) with increasing amplitude of loading and these values are plotted in Figure 9. Such degradation behaviour was caused by the bearing failure of the sheathing material surrounding screw heads leading to the formation of slots. Observations of stiffness degradations of the tested wall panels are summarized in two different aspects:

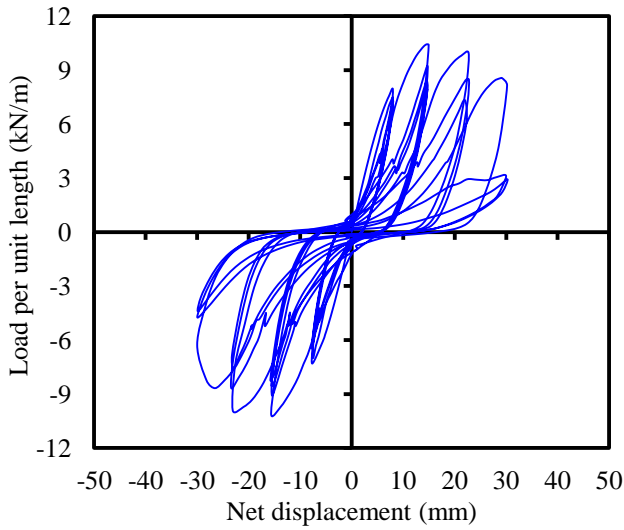
(a) Stiffness degradation with increasing displacement amplitude

Virgin Cycle-effective stiffness was degraded to about 30 to 40% till final phase of loadings whereas degradation was much higher (about 70%) for Last Cycle-effective stiffness. This was due to failure of wall panel at final phase of loading which is illustrated by a kink in Figures 9a and 9b. In contrast to effective stiffness degradation, secant stiffness degraded rapidly

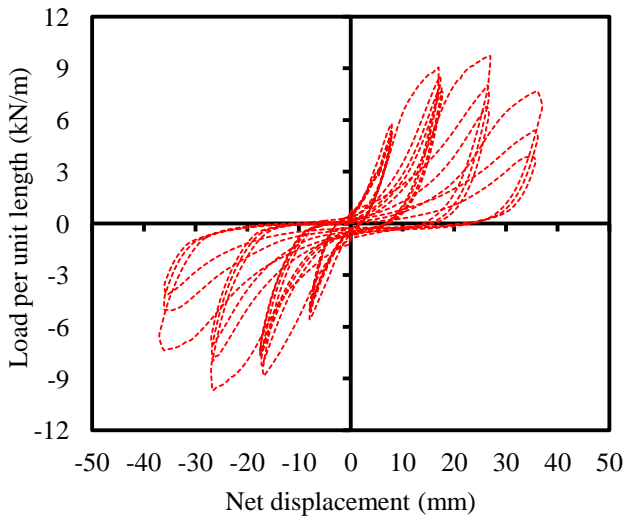
until final phase of loadings (about 70% for the Virgin Cycle and 80% for the Last Cycle). These charts clearly illustrate the softening of the structure with increasing displacement amplitude which result a period shift of about 2 to 3 times its initial natural period. These results confirmed the assumptions of the natural period shift made in developing a new loading protocol [10].

(b) Stiffness degradation from virgin cycle to last cycle at same displacement amplitude

There was a very little effective stiffness degradation (ranging from 2 to 11% for the first three phases of loadings) whereas more than 50% of the stiffness degraded at the final phase of loading due to failure of the wall panel. However, rate of secant stiffness degradation was found to be uniform (about 15 to 30% for the first three phases of loadings and 50% for the final phase of loading).



(a) Specimen FCB-Cyc-A



(b) Specimen FCB-Cyc-B

Figure 7: Load deflection behaviour of tested wall panels under cyclic loading

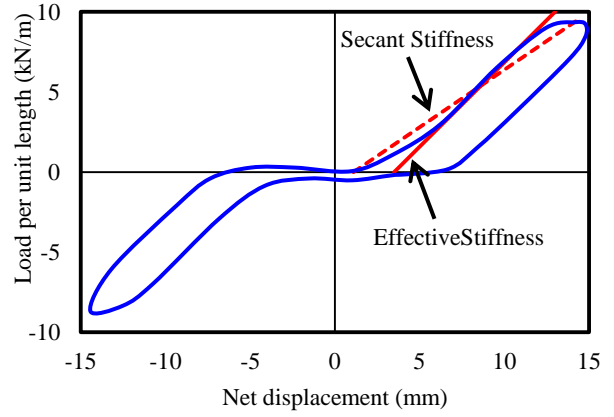
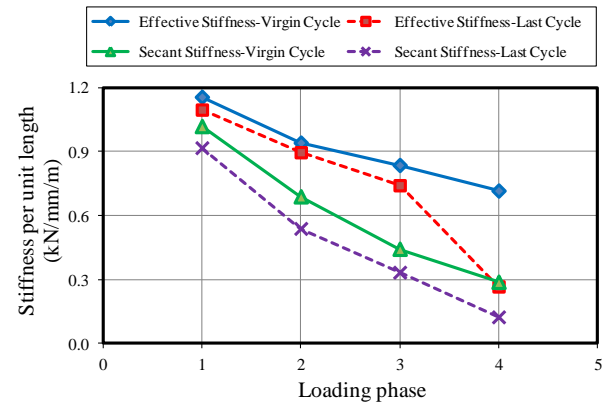
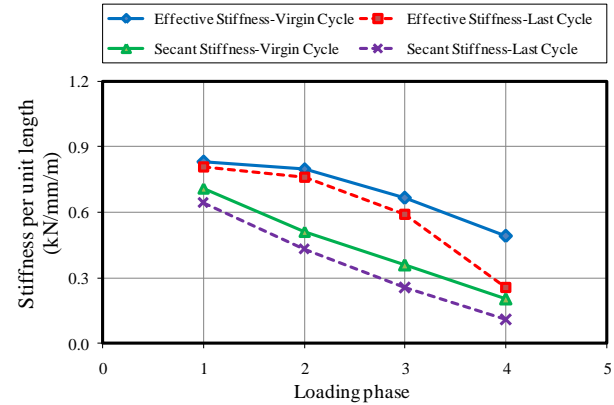


Figure 8: Definition of the effective and the secant stiffness for cyclic test [17]



(a) Specimen FCB-Cyc-A



(b) Specimen FCB-Cyc-B

Figure 9: Stiffness degradation (per unit length) of tested wall panels at different phases of cyclic loading

4 CONCLUSIONS

The paper presented experimental test results of cold-formed steel bracing wall panels with different aspect ratios with fibre cement board as sheathing material, subjected to in-plane monotonic and cyclic loadings. Four panels were tested under monotonic and cyclic loadings. The following conclusions were drawn from the test results:

- a) The failure modes of the wall panels were primarily due to failure of connections between the board and the CFS framing members. The sequence of failure modes of the tested wall panels was by corner cracking, bearing and screw head pull-through the board (BC+BB+BP) leading to the complete separation of the board from the framing member.
- b) Monotonic test results of the wall panels with different lengths (or aspect ratios) showed fairly similar load carrying capacity per unit length of wall panel. Hence, load carrying capacity of wall panels of intermediate lengths can be estimated using linear interpolations. However, the deflection capacity of a wall panel with shorter length (or larger aspect ratio) was found to be 20% higher compared to a wall panel with aspect ratio equal to 1.
- c) Cyclic test results showed a load degradation of less than 10% at the initial phase of loading and severe load degradation (about 50%) at the final phase of loading for both wall panels. With increasing amplitude of loading, secant stiffness degraded rapidly compared to effective stiffness at the initial phases of loadings whereas rate of stiffness degradations were much more severe at the final phase of loading (which was about 70% effective stiffness degradation and 80% secant stiffness degradations. Stiffness degradations provide clear information about the softening of the structure and for estimating a shift in the natural period of the structure.

ACKNOWLEDGEMENT

This research is funded by ARC Linkage Project LP110100430. The authors gratefully acknowledge the financial and technical support provided by the collaborating organisation, the National Association of Steel-framed Housing (NASH). Supply of materials and technical data by NASH members is also gratefully acknowledged.

REFERENCES

- [1] Tarpay T.S. Shear resistance of steel-stud wall panels. *Proceedings of the 5th International Specialty Conference on Cold-Formed Steel Structures*, 331-348, 1980.
- [2] Tarpay T.S. and Girard J.D. Shear resistance of steel-stud wall panels. *Proceedings of the 6th International Specialty Conference on Cold-Formed Steel Structures*, 449-465, 1982.
- [3] Serrette R.L. and Ogunfunmi, K. Shear resistance of gypsum-sheeted light gauge steel stud walls. *Journal of Structural Engineering*, ASCE, 122(4):383-389, 1996.
- [4] Serrette R.L., Encalada J., Juadines M. and Nguyen H. Static racking behaviour of plywood, OSB, gypsum and fiberbond walls with metal framing. *Journal of Structural Engineering*, ASCE, 123(8):1079-1086, 1997.
- [5] Landolfo R., Della C.G. and Fiorino L. Testing of sheathed cold-formed steel stud shear walls for seismic performance evaluation. *Proceedings of the 13th World Conference on Earthquake Engineering*, 2004.
- [6] Branston A.E., Chen C.Y., Boudreault F.A. and Rogers C.A. Testing of light-gauge steel- frame-wood structural panel shear walls. *Canadian Journal of Civil Engineering*, 33(5):561-72, 2006.
- [7] Moghimi H. and Ronagh R.H. Performance of light-gauge cold-formed steel strap-braced stud walls subjected to cyclic loading. *Engineering Structures*, 31(1):69-83, 2009.
- [8] Nithyadharan M. and Kalyanaraman V. Behaviour of cold-formed steel shear wall panels under monotonic and reversed cyclic loading. *Thin-Walled Structures*, 60:12-23, 2012.
- [9] Gatto K. and Uang C. Effects of loading protocol on the cyclic response of woodframe shearwalls. *Journal of Structural Engineering*, ASCE, 129(10):1384-1393, 2003.
- [10] Shahi R., Lam N., Gad E. and Wilson J. Protocol for testing of cold-formed steel wall in regions of low-moderate seismicity. *Earthquakes and Structures*, 4(6):629-647, 2013.
- [11] AS 1170.4. Structural design actions–Part 4: Earthquake actions in Australia. *Standards Australia*, 2007.
- [12] James Hardie Structural Bracing Manual, Australia. Available: <http://jameshardie.com.au/>, 2012.
- [13] BlueScope Steel, Available: <http://steelproducts.bluescopesteel.com.au/>.
- [14] Buildex Screw, Available: <http://buildex.com.au/>.
- [15] Herbert P.D. and King A.B. Racking resistance of bracing walls in low-rise buildings subject to earthquake attack (Vol. 2). *BRANZ Study Report SR78*, 1998.
- [16] NASH Standard. Residential and low-rise steel framing–Part 1: Design Criteria. National Association of Steel-framed Housing Inc, Australia, 2005.
- [17] Gad E.F., Duffield C.F., Hutchinson G.L., Mansell D.S. and Stark G. Lateral performance of cold-formed steel-framed domestic structures. *Journal of Engineering Structures*, 21(1):83-95, 1999.